DEVELOPMENT OF A VARIABLE-FREQUENCY RFQ LINAC FOR THE RILAC

O. Kamigaito, A. Goto, Y. Miyazawa, T. Chiba, M. Hemmi, S. Kohara,
M. Kase, Y. Batygin, Y. Yano,
The Institute of Physical and Chemical Research (RIKEN),
Wako-shi, Saitama 351-01, Japan

Abstract

A variable-frequency RFQ linac, based on a folded-coaxial resonator with a movable shorting plate, has been constructed as a new injector of the RIKEN heavy-ion linac (RILAC). The RFQ accelerates ions with mass-to-charge ratios of 6 to 26 at up to 450 keV per charge in the cw mode by varying its resonant frequency from 17.7 to 39.2 MHz. Stable operations have been achieved in the range of the acceleration voltage which covers the performance of the present Cockcroft-Walton injector. Acceleration tests have been successfully carried out using several kinds of ion beams from an 18GHz-ECRIS.

1 INTRODUCTION

A new injector of the RIKEN heavy ion linac (RILAC)[1] has been developed, which consists of an 18GHz-ECRIS and a variable-frequency RFQ linac, in order to meet the growing demand for more intensity of heavy ion beams. A real structure of the RFQ was constructed last year and has been tested. In this paper we describe some results obtained from the performance tests as well as the outline of the RFQ resonator.

2 RFQ RESONATOR

The RFQ resonator is based on a folded-coaxial structure[2]. The distinct features of this RFQ are that it can be operated in a low frequency region and the frequency range is quite large.

Figure 1 shows a schematic layout of the RFQ resonator. Horizontal vanes are held by front and rear supports fixed on the base plate. Vertical vanes are fixed on the inner surfaces of a rectangular tube which surrounds the horizontal vanes. This tube is supported by four ceramic pillars placed on the base plate. A stem suspended from the ceiling plate is in electric contact with the rectangular tube. A shorting plate placed around the stem can be moved vertically, which varies the resonant frequency. Radio-frequency power is capacitively fed through the side wall. A capacitive tuner is set on the other side and two capacitive pick-up monitors are on the base plate.

The lower stem illustrated in Fig. 1 is used only in high-frequency operations where it is in electric contact with both the conductor tube and the base plate, while it is detached from the tube in low-frequency operations. This stem was found to reduce the power consumption because it shares the rf electric current with the upper stem[3].

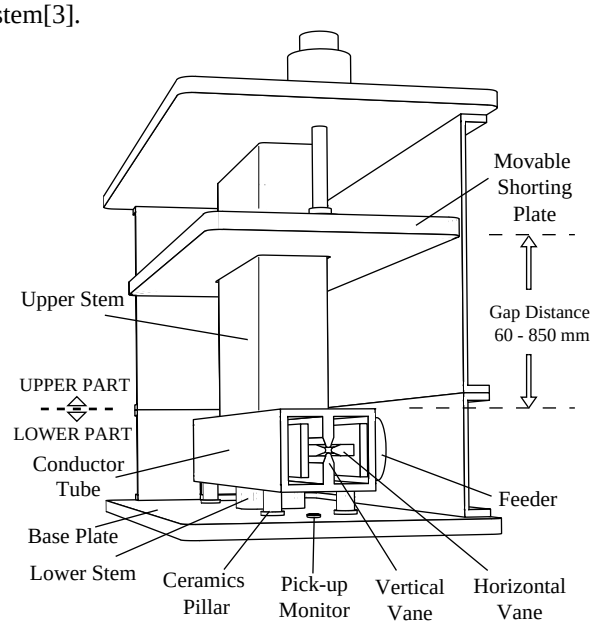

Figure 1. Schematic drawing of the RFQ resonator. The inner volume of the resonator is about 1700 mm (length) × 700 mm (width) × 1150 mm (height).

The resonator is separable into upper and lower parts, as shown in Fig. 1. The horizontal vanes and the rectangular tube with the vertical vanes are rigidly fixed inside the lower part. The upper part containing the stem and the movable shorting plate can be removed as a unit. This separable structure permits accurate alignment of the vanes and easy maintenance.

The channels for water cooling have been designed based on the heat analysis. Water for the horizontal vanes is supplied through the front and rear supports of the vanes. That for the vertical vanes and the rectangular tube is provided through the inside of the upper stem. The total water flow is 155 *l*/min of 7 atm. Two turbo-molecular pumps (1500 *l*/s) are fixed on both sides of the resonator.

The vanes have been three-dimensionally machined within the accuracy of ±50 μm. The vane parameters have been determined by taking the results of a numerical simulation into account[4]. Misalignment effect on the beam transmission efficiency have also been examined[4].

3 PERFORMANCE TESTS

3.1 Low power tests

Figure 2 shows the measured resonant frequency along with the values calculated by the MAFIA program. The horizontal axis represents the gap distance between the top surface of the conductor tube and the bottom surface of the shorting plate. The resonant frequency varies from 17.7 to 39.2 MHz by changing the position of the shorting plate by a stroke of 790 mm.

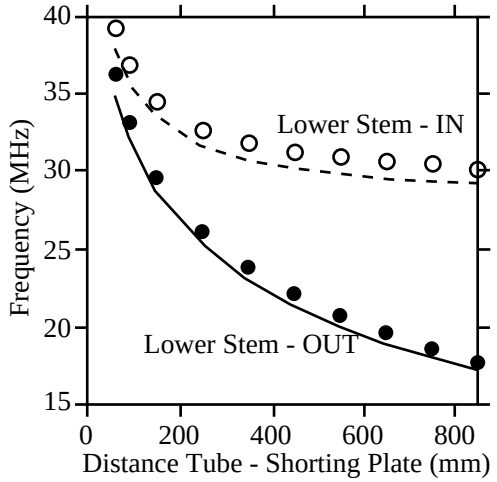

Figure 2. Measured resonant frequency along with the MAFIA calculations. The closed circles and the solid curve represent the measured and the calculated values, respectively, when the lower stem is not used. The open circles and the dashed curve represent the measured and the calculated values, respectively, when the stem is used.

Figure 3 shows the measured Q-values and shunt impedances. The corresponding MAFIA-calculation curves are shown in the figures as well. The shunt impedance R_S is defined by $V^2/(2P)$, where P is the rf power consumption and V is the intervane voltage. As shown in the figure, the measured Q-values and shunt impedances with the lower stem are larger than those without the stem above 30 MHz.

The MAFIA calculations overestimate the measured values by about 50 %. This is considered to result from the fact that the calculation does not realistically treat the roughness of the wall surface and the imperfection of the electric contact.

The power losses estimated from the shunt impedances are 6 kW at 17.7 MHz and 26 kW at 39.2 MHz for the maximum intervane voltage of 33.6 kV in the cw operation.

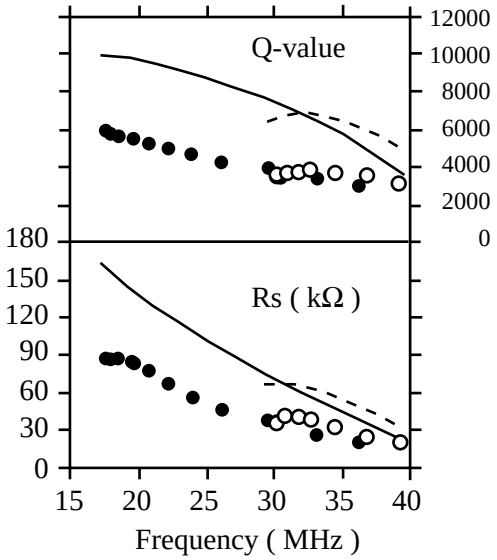

Figure 3. Measured Q-values and the shunt impedances along with the MAFIA calculations. The data of symbols and curves are obtained under the same conditions as in Fig. 2.

3.2 High power tests

High power tests have been performed with an rf power source based on an Eimac 4CW50000E, which has a cw power of 40 kW at maximum between 16.9 MHz and 40 MHz.

In the first stage of the tests we encountered a problem on the ceramics pillars. When the intervane voltage was above 25 - 30 kV, the pillars were broken by the heat due to the dielectric losses around the metal screws fixing the pillars to the conductor tube.

This problem has been solved by adopting the structure illustrated in Fig. 4, which consists of Al_2O_3 welded with copper-tungsten metal on its both sides. This welding is possible because both materials have similar coefficients of the linear thermal expansion. After this improvement, the RFQ has been stably operated in the whole range of the acceleration voltage acceptable by the RILAC. The vacuum stays in a range of $1 - 3 \times 10^{-7}$ Torr at a pump head. No significant temperature-rise has been detected during the operation.

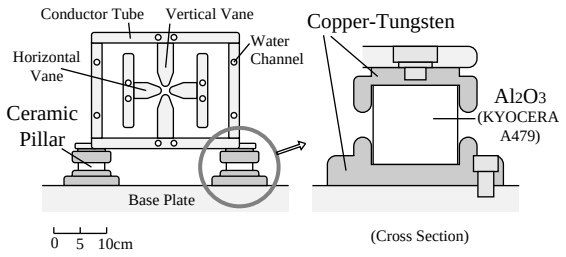

Figure 4. Schematic drawing of the ceramic pillar.

3.3 Acceleration tests

Acceleration tests have been performed using beams from an 18GHz-ECRIS. Figure 5 shows the schematic drawing of the beam line. The extracted beam from the ion source is focused by Einzel lens and is bent by a bending magnet. The bending magnet also has a focusing function by the slant pole edges. The beam is focused again by a solenoid lens before entering the RFQ. The diagnostic boxes contain Faraday cups, profile monitors, emittance monitors, and slits. Three capacitive pick-up probes are used for the TOF measurement of the beam velocity.

The accelerated ions so far are $O^{3,4,5+}$, Ne^{4+}, $Ar^{2,3,6,8,9,11+}$, Kr^{9+}, Xe^{12+}, $Ta^{7,16,17+}$ at the frequencies of 17.7, 19.5, 26.1, 29.5, 32.8, 34.4, 36.8 and 39.2 MHz in the range of the intervane voltage of 17 - 35 kV. The maximum transmission efficiency, defined by the ratio of the beam current in two Faraday cups (FC1 and FC2 in Fig. 5), was 88 % with the beam intensity of 120 eμA. The velocity of the output beam measured by the TOF method is in agreement with the designed value within 1 %.

The input beam emittance from the ion source is 150 - 300 π mm•mmrad, which depends both on the charge states of the ion and the extraction voltage. Measurements of the emittance and the energy distribution of the accelerated beam are in preparation.

4 INSTALLATION PLAN

The new injector will be installed in the RILAC beam line in this summer. At the same time, the maximum voltage of the ECRIS is raised to 20 kV. New vanes are under fabrication so that the RFQ can accept the upgraded beams. Acceleration tests of the RILAC with the new injector will be completed by the end of this year.

5 ACKNOWLEDGMENT

The authors are grateful to Dr. N. Tokuda and Dr. S. Arai at INS for the usage of vane-cutting program as well as for the fruitful information about the vane design. The resonator was fabricated by Sumitomo Heavy Industries, Niihama Work, and the rf power source by Denki Kogyo.

REFERENCES

[1] M. Odera, Y. Chiba, T. Tonuma, M. Hemmi, Y. Miyazawa, Y. Inoue, T. Kambara, M. Kase, T. Kubo, and F. Yoshida, Nucl. Instrum. and Methods, **227**, 187 (1984).

[2] O. Kamigaito, A. Goto, Y. Miyazawa, T. Chiba, M. Hemmi, M. Kase, and Y. Yano, Jpn. J. Appl. Phys. **33**, L537 (1994).

[3] O. Kamigaito, A. Goto, Y. Miyazawa, T. Chiba, M. Hemmi, S. Kohara, M. Kase, and Y. Yano, Jpn. J. Appl. Phys. **34**, 5799 (1995).

[4] Y. Batygin, A. Goto, O. Kamigaito, and Y. Yano:, RIKEN Accel. Progr. Rep. 28, p.172 (1994) and in this proceeding.

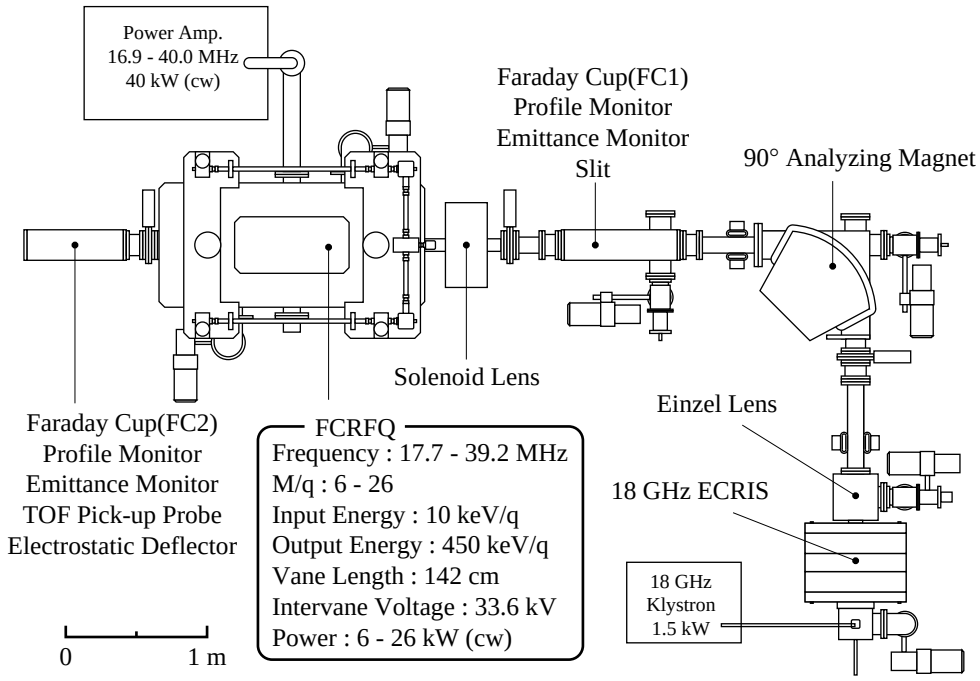

Figure 5. Schematic layout of the beam line.